See related commentary on pg 1059

ORIGINAL ARTICLE

An Extended Epidermal Response Heals Cutaneous Wounds in the Absence of a Hair Follicle Stem Cell Contribution

Abigail K. Langton[1], Sarah E. Herrick[2] and Denis J. Headon[1]

Hair follicles have been observed to provide a major cellular contribution to epidermal healing, with emigration of stem-derived cells from the follicles aiding in wound reepithelialization. However, the functional requirements for this hair follicle input are unknown. Here we have characterized the keratinocyte stem cell status of mutant mice that lack all hair follicle development on their tail, and analyzed the consequent alterations in epidermal wound healing rate and mechanisms. In analyzing stem cell behavior in embryonic skin we found that clonogenic keratinocytes are relatively frequent in the ectoderm prior to hair follicle formation. However, their frequency in the interfollicular epidermis drops sharply by birth, at which time the majority of stem cells are present within the hair follicles. We find that in the absence of hair follicles cutaneous wounds heal with an acute delay in reepithelialization. This delay is followed by expansion of the region of activated epidermis, beyond that seen in normal haired skin, followed by appropriate wound closure.

JID JOURNAL CLUB ARTICLE: For questions, answers, and open discussion about this article please go to http://network.nature.com/group/jidclub

Journal of Investigative Dermatology (2008) **128,** 1311–1318; doi:10.1038/sj.jid.5701178; published online 22 November 2007

INTRODUCTION

The most obvious function of a hair follicle (HF) is to produce a hair fiber, but it has long been noted that follicles also contribute to healing of injured skin. Wounds that remove the surface epidermis but leave HFs relatively intact are reepithelialized simultaneously across the entire wound, with patches of new epidermis seen spreading outwards from the necks of the HFs. In contrast, deep wounds that destroy the HFs are slower to heal and do so only from the margins (Bishop, 1945). Recognition of these different healing modes has led to a realization that wound depth is critical when treating burn cases, with shallow wounds left to reepithelialize of their own accord, while deep wounds typically receive grafts of surface epidermis from uninjured sites (Papini, 2004).

Consistent with their role as a repair reservoir, HFs maintain a variety of the skin's stem cells, including those of both the keratinocyte (Cotsarelis, 2006) and melanocyte (Nishimura *et al.*, 2002) lineages. These stem cell populations reside a specialized niche in the lower permanent region of the HF, termed the bulge, protected well below the skin surface. The keratinocyte stem cells fuel cyclical HF and hair growth through life (Morris *et al.*, 2004) and their progeny contribute to the interfollicular epidermis (IFE) during wound repair, though they are not involved in maintaining homeostasis in intact skin (Ito *et al.*, 2005; Levy *et al.*, 2005). There appear to be several distinct epidermal stem and progenitor cell populations within the HF, with progenitor cells residing in the infundibulum of the upper follicle (Nijhof *et al.*, 2006), in addition to the well-characterized and slightly deeper bulge stem cells. Emigration of cells from the HF to the IFE has been observed in wounded mouse skin using DNA synthesis labels to tag the rapidly dividing cells of the upper HF (Taylor *et al.*, 2000). More recently, cre recombinase-based lineage tracing has been used to label either the bulge stem cells and their progeny in the lower follicle using the *Keratin15* promoter (Ito *et al.*, 2005), or the entire follicle, including most of the upper infundibular region, using the *Shh* promoter (Levy *et al.*, 2005). These approaches have found that following wound healing between 25 and 50% of cells in the repaired IFE are of HF origin (Ito *et al.*, 2005; Levy *et al.*, 2005, 2007); however, the functional requirement for this HF cell contribution and the consequences of its absence are unknown.

HF primordia are produced during embryonic development via a series of epithelial–mesenchymal interactions. The sites of HF formation first become morphologically distinct as a thickened placode of epithelial cells. This placode grows down into the underlying dermis, undergoes differentiation, and ultimately produces a hair fiber (Fuchs, 2007). On mouse trunk skin initiation of HF development occurs in three temporally distinct waves: with primary HFs initiated at

[1]*Faculty of Life Sciences, University of Manchester, Manchester, UK and* [2]*School of Medicine, Faculty of Medical and Human Sciences, University of Manchester, Manchester, UK*

Correspondence: Dr Denis J. Headon, Faculty of Life Sciences, University of Manchester, Oxford Road, Manchester M13 9PT, UK.
E-mail: denis.headon@manchester.ac.uk

Abbreviations: Eda, ectodysplasin; Edar, Eda receptor; Edaradd, Edar-associated death domain; HF, hair follicle; IFE, interfollicular epidermis; LRC, label-retaining cell; WT, wild type

Received 23 July 2007; revised 4 September 2007; accepted 26 September 2007; published online 22 November 2007

embryonic day 14 (E14), secondary HFs at E16, and tertiary HFs around birth. On the tail only primary HFs develop, with their formation starting at E16. A number of molecules are known to be involved in regulating HF fate specification and morphogenesis (Fuchs, 2007), with some factors playing roles that are restricted to a subset of follicle types. Mutations that impair the Eda receptor (Edar) signaling pathway, composed of the ligand ectodysplasin (Eda), its receptor Edar, and the cytoplasmic signaling adapter Edar-associated death domain (Edaradd), result in a complete absence of primary HFs, though secondary HFs do develop (Headon *et al.*, 2001). Thus mutations affecting components of this pathway yield an adult mouse with secondary HFs on the trunk and a complete absence of HFs on the tail.

We have addressed the functional roles of HF-derived cells in wound healing using *Edaradd* mouse mutants with developmental defects in HF formation. The tail skin of these mutants provides a model that entirely lacks all classes of cutaneous adnexae, such as HFs, scales, and eccrine sweat glands, to study the repair capacity of IFE in isolation. Initially we characterized the epidermal stem cell status of *Edaradd* mutant tail skin through development and into adult life. We then wounded this skin to analyze the effects of a lack of HF-associated stem cells on epidermal repair rate and mechanisms. We find that HF-derived cells aid in rapid epidermal production to aid acute wound closure, but that their absence is circumvented by the IFE, which recruits a larger area of epidermis when delayed healing becomes manifested.

RESULTS

Stem cell behavior is exhibited by embryonic epidermis but is largely lost from IFE before birth

Prior to addressing the role of HFs in wound repair, we characterized the *Edaradd*$^{cr/cr}$ tail epidermis to determine its suitability as a model of normal IFE that lacks all skin appendages. Initially we assayed epidermal stem cell characteristics and behavior during prenatal development. Our analysis of known stem cell and niche markers failed to detect localized staining until postnatal day 5 (P5)–P10, when these markers were associated with well-developed HF bulges (Figure S1). Therefore, to estimate stem cell frequency in embryonic skin we exploited the well-characterized ability of keratinocyte stem cells to produce colonies when cultured for 2 weeks on an irradiated fibroblast feeder layer (Rheinwald and Green, 1975; Morris and Potten, 1994; Blanpain *et al.*, 2004). We first detected Keratin 14 (K14)-positive epidermal colonies produced by cells from E7 embryos (Figure 1a), prior to expansion of the ectoderm across the embryo's surface. As the skin proper begins differentiation, the colony-forming potential of *Edaradd*$^{cr/cr}$ mutant tail epidermis, in which tail HFs never form, was compared to that of *Edaradd*$^{cr/+}$ littermates (Figure 1b and c). In control tail skin the frequency of clonogenic keratinocytes is fairly constant from E15 to P50, with a transient peak at E17 as HF downgrowth is underway. In mutant epidermis, clonogenic activity is identical to that of normal skin until E16, after which it drops precipitously and remains very low thereafter. Between E17 and E18 the reduction in colony forming activity in control and mutant skin is of the same absolute magnitude, suggesting that the clonogenic population present in the epidermis prior to HF formation is lost as a consequence of the age of the skin and occurs independently of follicle development.

Edaradd mutant animals entirely lack HFs on the tail, and on the trunk do not form primary hair placodes from E14 to E16, but do develop secondary HFs from E17 to birth (Figure 1d). To determine whether the findings from tail skin also apply to the trunk skin we determined colony-forming ability of cells from the dorsum of mutant and heterozygous embryos. We found that during primary HF development in normal E15 trunk skin there are many more stem cells than in *Edaradd*$^{cr/cr}$ mice, which lack placodes at this age. By E18, when both mutant and wild-type (WT) skins are producing secondary HFs, their stem cell frequencies are comparable (Figure 1e).

As normal tail epidermis has much higher stem cell activity than mutant from E18, when normal skin contains HF buds, we determined whether these clonogenic cells were located in the follicle primordia themselves, or were present in the IFE and maintained there by the influence of the HFs. E18 tail skin was separated into HF and IFE fractions (Figure 1f) and clonogenic activity assessed in each cell fraction. We found that almost all colony-forming cells reside within the HFs, while stem cell frequency in the IFE is similar to that of mutant skin (Figure 1g). Together, these results indicate that a pre-follicle stem cell population is present in the epidermis until just before birth, and that HF primordia generate their own clonogenic cells as they begin to undergo morphogenesis. Hence, during prenatal life the stem cell behavior displayed by *Edaradd*$^{cr/cr}$ tail epidermis mirrors that seen in WT IFE, including a sharp reduction in clonogenic potential just before birth.

A long lived IFE stem cell population is produced and maintained independently of HF formation

Next we examined adult *Edaradd*$^{cr/cr}$ epidermis to determine whether it possesses the stem cell characteristics and behavior of normal IFE. We found that tail epidermis from 100-day-old mutant mice had a very low clonogenic activity, at about 2.5% that of controls (Figure 2a). In adult mice, administration of a pulse of BrdU followed by a chase period of several weeks leaves only the relatively quiescent stem cells labeled (Cotsarelis *et al.*, 1990). Using this method BrdU label-retaining cells (LRCs) were readily detected in HFs of the dorsal trunk in both heterozygous control and mutant animals, demonstrating that Edar pathway function is not directly required for generating or maintaining an LRC population (Figure 2b and c). As in the dorsal skin, in normal tail skin the majority of LRCs lay within HFs, though isolated LRCs in the basal layer of the IFE were also present (Figure 2d). Such isolated LRCs were also detected in mutant tail skin (Figure 2e) at a frequency not significantly different from that of control IFE (Figure 2g). Using the *Dct::lacZ* transgenic line (Mackenzie *et al.*, 1997) we confirmed that these tail IFE LRCs are not melanocyte stem cells (Figure 2f) consistent with their possessing a keratinocyte identity. Despite both cell kinetic and clonogenic behavior strongly indicating the presence of relatively rare stem cells in mutant

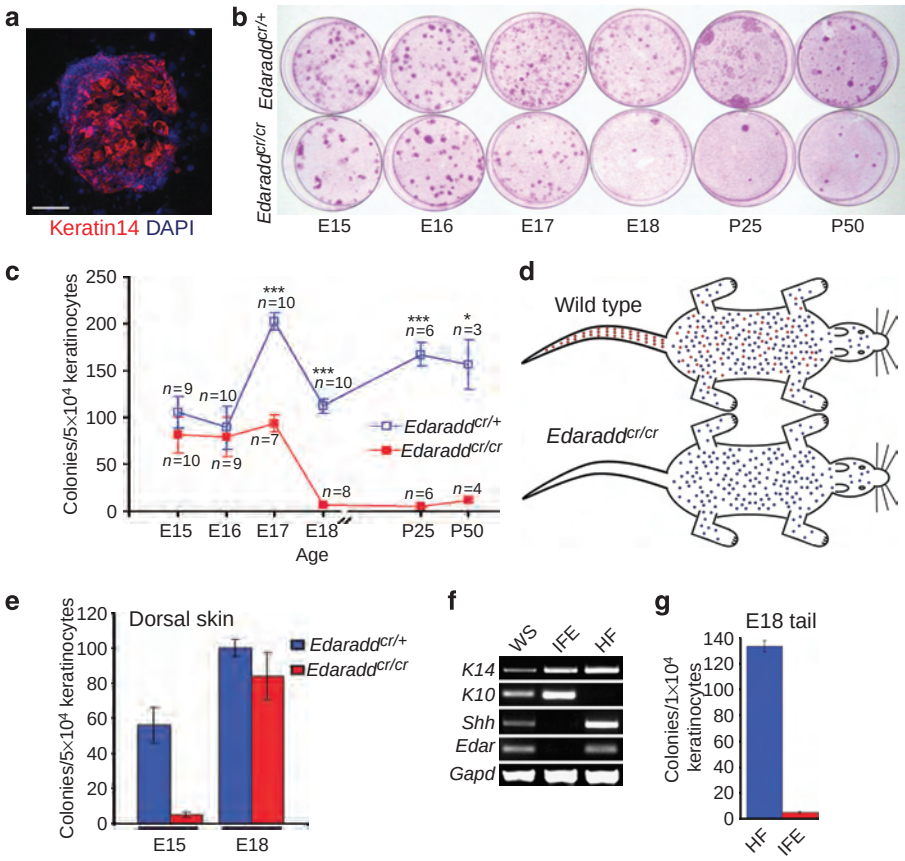

Figure 1. Prenatal origins of epidermal stem cells. (**a**) K14-positive colony produced by cells from a dissociated E7 embryo. Bar = 250 μm. (**b**) Keratinocyte colonies from tail epidermis of *Edaradd*$^{cr/cr}$ and control *Edaradd*$^{cr/+}$ littermates from E15 to P50. (**c**) Quantification of clonogenic potential in tail epidermis from E15 to P50. Error bars show SEM. (**d**) Schematic of the WT and *Edaradd*$^{cr/cr}$ phenotypes. Red dots indicate primary HFs, forming on the body between E14 and E16, and from E16 on the tail. Primary follicles do not develop in the *Edaradd*$^{cr/cr}$ mutant. Blue dots indicate secondary follicles, forming on the trunk, but not the tail, from E17 to birth. Approximately 5% of HFs on the trunk of an adult mouse are primary follicles. (**e**) Colony-forming potential of embryonic dorsal epidermis from *Edaradd*$^{cr/cr}$ and control *Edaradd*$^{cr/+}$ littermates at E15 and E18. (**f**) RT-PCR validation of whole skin (WS), IFE, and HF isolation using the generic basal keratinocyte marker *Keratin14*, IFE maker *Keratin10*, HF markers *Shh* and *Edar*, and *Gapd* control. (**g**) Colony-forming potential of E18 WT tail HF epithelium and IFE. Error bars indicate SEM. *$P<0.05$; ***$P<0.001$.

tail skin, we did not detect localized expression of bulge stem cell markers or localized niche markers in these samples (Figure 2h–o). Together, these assays indicate that IFE LRCs and clonogenic cells are produced independently of HF formation and that there is no compensatory increase in the frequency of such cells in the absence of HFs. Confirmation that the stem cells status of adult *Edaradd* mutant epidermis accurately reflects that of normal IFE allowed us to use this model to address the role of HF-derived cells in skin wound healing.

HFs contribute to the acute wound healing response

A major component of the wound healing process is the restoration of an epidermal barrier by growth and migration of the continuous epithelial sheets adjacent to the wound and by emigration of HF cells to the skin surface (Li *et al.*, 2007). The absence of an HF stem cell reservoir in the *Edaradd*$^{cr/cr}$ mutant allowed us to directly address the functional role of bulge-derived cells in wound repair. We made full thickness incisional wounds on the tail (Figure 3a–h) and dorsum of control and *Edaradd*$^{cr/cr}$ mice and measured the rate of epidermal closure. We did not observe any differences between genotypes in healing of the haired trunk skin, indicating that Edaradd does not play a direct role in wound healing (Figure S2). On the tail, we found that wounds in WT skin closed steadily from 3 to 6 days post-wounding. Wounds in mutant tail skin were of the same dimension as WT at 3 days post-wounding, but displayed essentially no closure to day 4 (Figure 3a–f and i). This acute delay in reepithelialization was resolved by 6 days post-wounding, when closure was complete in skin of mutant and control animals (Figure 3c, g, and i). We did not observe differences in dermal healing mechanisms or the degree of inflammatory infiltrate between genotypes in wounds on back or tail skin. Thus in the absence of an HF input there is an acute delay in wound reepithelialization from which the epidermis recovers to cover the damaged region.

Lack of HFs results in an extended epidermal wound response

To evaluate the mechanisms of epidermal repair in mutant tail skin, we analyzed expression of K6, a marker of activated

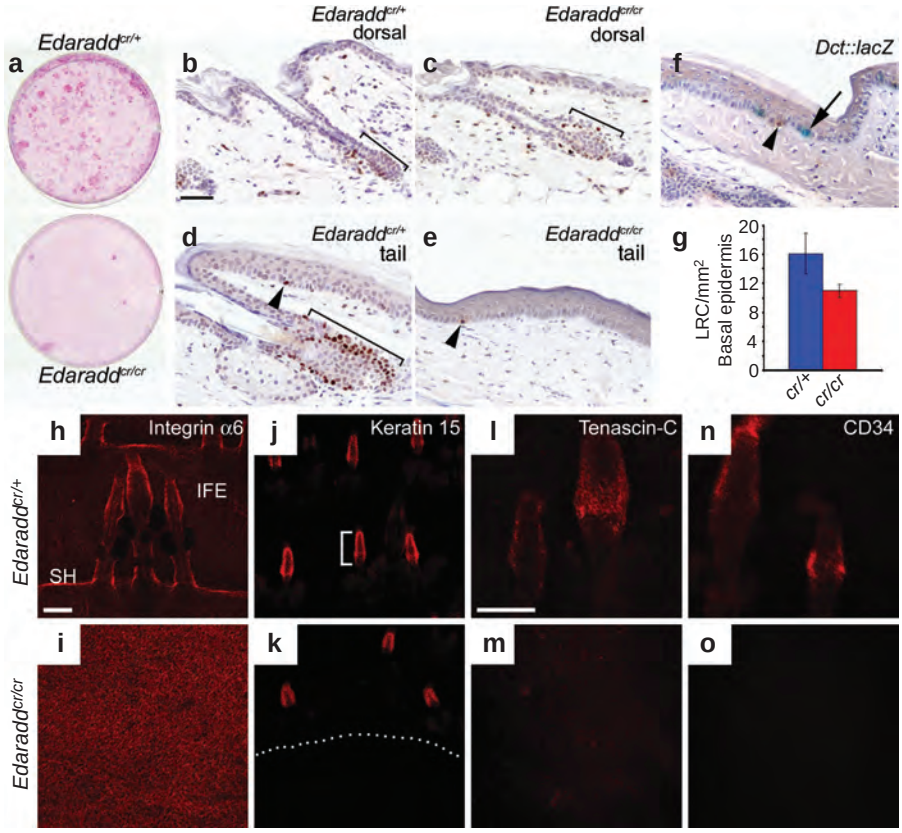

Figure 2. Epidermal stem cells in the absence of HF niches. (**a**) Colony-forming potential of P100 *Edaradd*$^{cr/cr}$ and *Edaradd*$^{cr/+}$ tail epidermis. (**b–e**) BrdU LRCs are found in the bulge region of HFs in P100 dorsal trunk skin (**b** and **c**, bracket) of mutant and control mice. HFs of control tail contain LRCs (**d**, bracket), and isolated LRCs (arrowheads) are found in the basal layer of the epidermis in both control (**d**) and mutant (**e**) tail skin. Bar = 50 μm. (**f**) *Dct::lacZ*-positive cells of the melanocyte lineage (arrow) are distinct from the LRCs detected in the basal IFE (arrowhead). (**g**) Quantification of IFE LRCs/mm^2 of *Edaradd*$^{cr/cr}$ and *Edaradd*$^{cr/+}$ tail epidermis ($P > 0.2$). Error bars show SEM. (**h–o**) Whole-mount immunodetection of stem cell and HF bulge markers in P35 tail epidermis. *Edaradd*$^{cr/cr}$ epidermis broadly expresses integrin α6, but does not express the stem cell markers K15, Tenascin-C, or CD34 (**i, k, m, o**). In mutant skin at the point of tail attachment to the trunk (**k**, dotted line), secondary HFs exhibit K15 expression in a pattern identical to that seen in control tail follicles (**j**). Bar = 100 μm. SH = scale hinge.

IFE responding to a wound (Coulombe, 2003). At 3 days post-wounding the extent of K6 expression from the wound edge (Figure 4a, e, and i) and the thickness of K6-positive suprabasal epidermis (Figure 4a, e, and j) were identical in IFE adjacent to wounds of both genotypes. However, at days 4 and 6, when delayed closure is apparent in *Edaradd*$^{cr/cr}$ (Figure 3i), both the extent from the wound edge and the thickness of K6 expression were greater in mutant skin than control (Figure 4b, c, f, g, i, and j). By 8 days post-wounding, when epidermal closure is complete, K6 expression characteristics were again similar for both genotypes (Figure 4d and h–j). Immunodetection of proliferating cell nuclear antigen (PCNA) agreed with the K6 results in that the epidermal hyperproliferative response also extended farther into the suprabasal epidermis and to a greater distance from the wound edge in mutant than in control skin (Figure 4k–r), though the peak in extent of suprabasal PCNA was slightly delayed relative to that of K6 (Figure 4s). These experiments demonstrate that follicle-derived cells enhance early stages of wound closure and that in the absence of this HF contribution an expanded area of IFE is recruited to achieve reformation of the epidermal barrier.

DISCUSSION

In exploring the role of HF-associated stem cells in wound healing, we used the *Edaradd*$^{cr/cr}$ mutant tail to model skin lacking all appendages that could provide keratinocytes to damaged IFE. In order to draw firm conclusions from this model system about the role of HFs in healing it was important to ensure that (i) *Edaradd*$^{cr/cr}$ mutant epidermis has the characteristics of WT IFE, and (ii) that *Edaradd* has no direct role in regulating stem cell behavior or wound healing. We compared the stem cell characteristics of mutant tail epidermis to WT IFE and found no significant difference in developmental course or adult condition between genotypes. In addition, we performed clonogenic, BrdU label retention, and wound healing assays on the haired mutant trunk skin. The results obtained did not differ from those of WT skin, allowing us to conclude that the effects we observe are indeed a secondary result of the absence of HF niches, and are not primarily caused by impaired Edaradd function.

During epidermal development we find that stem cell behavior is exhibited prior to the onset of HF formation, though this high clonogenic potential of the IFE is greatly decreased just before birth. The appearance of HF primordia

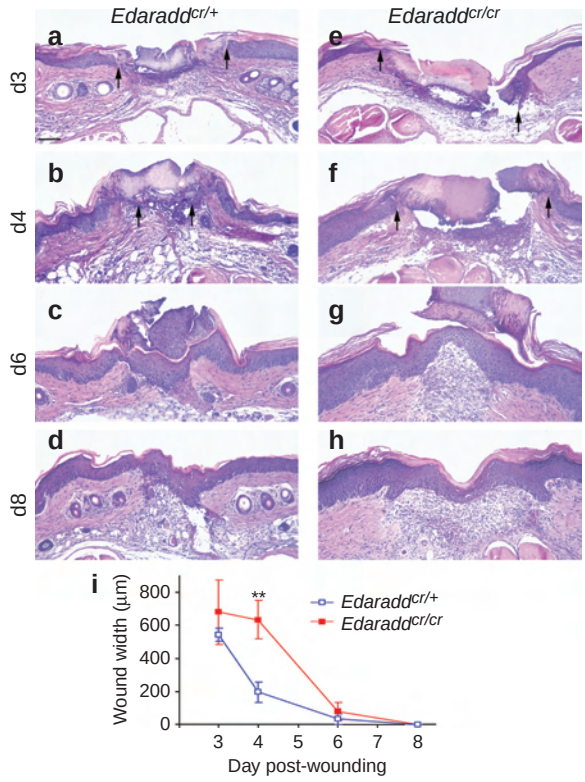

Figure 3. Wound reepithelialization in skin lacking HFs undergoes an acute delay followed by completion of repair. (**a**–**h**) Hematoxylin- and eosin-stained cross-sections of full thickness incisional wounds made in *Edaradd*$^{cr/+}$ (**a**–**d**) and *Edaradd*$^{cr/cr}$ (**e**–**h**) tail skin. (**a**, **e**) Day 3, (**b**, **f**) day 4, (**c**, **g**) day 6, (**d**, **h**) day 8 post-wounding. Arrows indicate epidermal leading edges. Bar = 100 μm. (**i**) Quantification of wound widths in *Edaradd*$^{cr/cr}$ and *Edaradd*$^{cr/+}$ littermates from 3 to 8 days post-wounding. Error bars show SEM.

increases stem cell potential, probably as a result of the complex molecular influences that generate the HF placode (Schmidt-Ullrich and Paus, 2005; Rhee *et al.*, 2006; Fuchs, 2007). After birth the majority of epidermal stem cells reside within the HFs; we found that HF-deficient tail skin has a clonogenic potential of about 2.5% than that of normal skin, and that the frequency of BrdU LRCs in hairless skin is reduced to approximately the same extent (we found 16 LRCs/mm^2 IFE, while approximately 650 LRCs reside within HFs in this area; Braun *et al.*, 2003). This congruence agrees with reports that epidermal LRCs, though quiescent *in vivo*, are the population that produces colonies *in vitro* (Morris and Potten, 1994). It has recently been reported that normal epidermal homeostasis does not rely on a specialized stem cell (Clayton *et al.*, 2007), indicating that the LRCs we detect may be quiescent until an appropriate stimulus, such as wounding, occurs.

During wound repair, we find that HFs contribute to rapid epithelial closure. In isolation, mutant IFE shows delayed healing at 4 days post-incision. This agrees with the observation of cells of HF origin arriving in a wound between 2 and 4 days post-incision (Ito *et al.*, 2005). The absence of this HF input leads to recruitment of epidermal cells from a wider field around the lesion, suggesting that recruitment of IFE to wound repair expands until a sufficient overall response is mounted. Thus, during wound healing in haired skin the extent of responding IFE is normally limited by the provision of cells from the HFs.

In our experimental model the entire pilosebaceous unit is absent, removing all HF contributions to wound healing. The observed heterogeneity in epidermal stem cells within the adult bulge itself (Blanpain *et al.*, 2004), as well as the presence of a distinct progenitor cell population in the infundibulum (Nijhof *et al.*, 2006), means that we detect the net effect of removal of all of these potential inputs. The individual roles of each HF stem or progenitor cell type in cutaneous healing remains to be dissected.

In all, HFs provide a measurable contribution to the rate of reepithelialization from a wound margin, but this input is not essential for the healing of incisional wounds. It is possible, however, that severe wounds requiring massive epidermal repair would require HF stem cells to produce epidermis over an extended healing period. In addition to accelerating ingrowth at epidermal leading edges, as we demonstrate here, evenly spaced HFs provide islands of epidermal repair capacity in case of destruction limited to the surface epithelium. It is likely that their scattered distribution, in addition to any intrinsically superior repair ability, makes HF-derived cells such important agents in healing burn wounds.

Many growth factors that play roles in cutaneous wound healing have been identified, with fibroblast growth factor signaling known to play a key role in stimulating epithelial proliferation at the wound edge (Werner *et al.*, 1994), and heparin-binding-EGF regulating epidermal cell migration (Shirakata *et al.*, 2005). Recently, it has been shown that keratinocytes must express c-Met to contribute to wound healing, suggesting that its ligand, HGF/SF, may be a major mitogen and chemoattractant during wound repair (Chmielowiec *et al.*, 2007) and could have a role in drawing cells out of the HFs during this process. Whether these, and many other (Werner and Grose, 2003), molecules known to be involved in reepithelialization preferentially regulate either HF-derived cells or keratinocytes of the IFE remains to be determined. Dissection of the possibly distinct molecular mechanisms that regulate the IFE and HF cellular inputs during wound healing will aid in our understanding of cutaneous repair and possibly in targeting therapies to accelerate and improve the outcome of this process.

MATERIALS AND METHODS

Animals

Experimental animals were obtained from *Edaradd*$^{cr/cr}$ × *Edaradd*$^{cr/+}$ or *Eda*$^{Ta/Ta}$ × *Eda*$^{Ta/Y}$ crosses. The *Dct::lacZ* line was provided by Ian Jackson (Medical Research Council Human Genetics Unit, Edinburgh, UK). For timed matings, the day on which a vaginal plug was detected was designated day 0.

PCR

For RT-PCR, RNA was isolated using TRI Reagent (Sigma, St Louis, MO) and reverse transcribed using random primers and AMV RT (Roche, Mannheim, Germany) in a 20 μl reaction. Reactions were

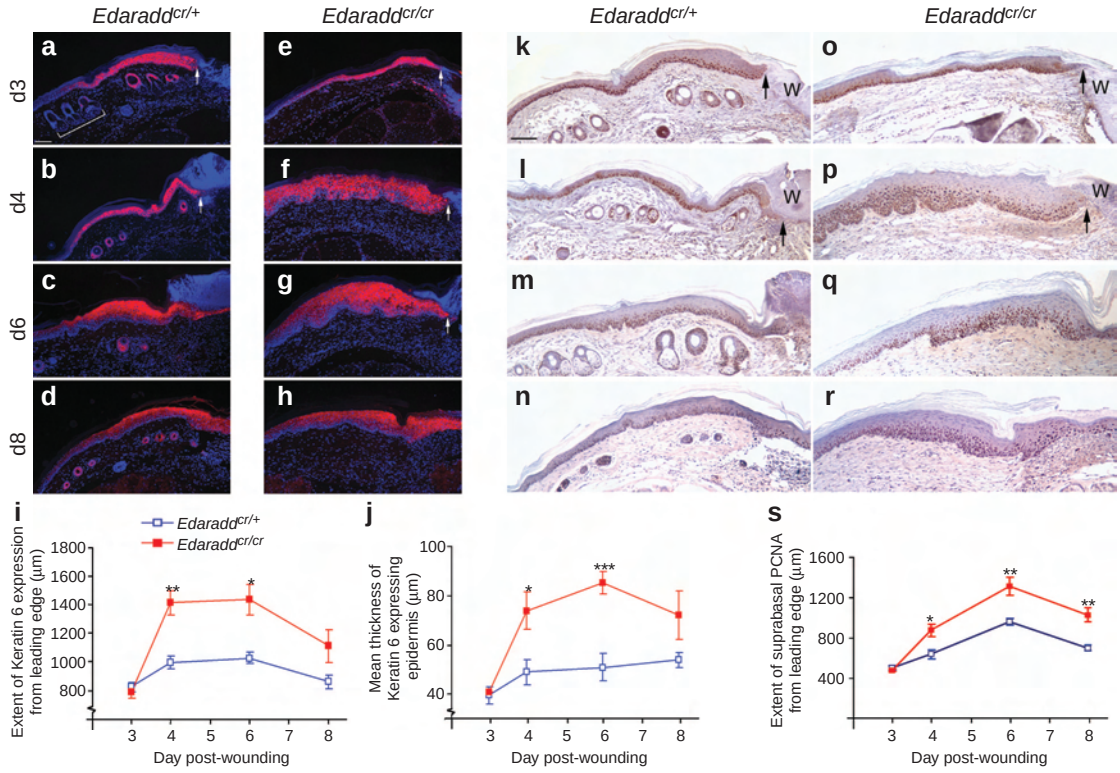

Figure 4. An extended epidermal response occurs to heal wounds in tail skin lacking HFs. (**a–h**) Expression of K6 adjacent to tail incision wounds from 3 to 8 days post-wounding shows alteration of the extent and thickness of responding epidermis in mutant skin (**e–h**) compared to control littermates (**a–d**). Arrows point to epidermal leading edge at the wound margin. Bar = 100 μm. (**i**, **j**) Quantification of extent from the wound edge (**i**) and mean thickness (**j**) of K6 expressing epidermis. (**k–r**) Analysis of cell proliferation determined by PCNA staining. PCNA-positive cells are distributed at a greater distance from the wound edge and in a greater proportion of the suprabasal epidermal layers in mutant mice (**o–r**) than control littermates (**k–n**). Arrows point to leading edge, W: wound. Bar = 100 μm. (**s**) Quantification of the extent of suprabasal PCNA-positive keratinocytes away from the wound margin. Error bars show SEM. $*P<0.05$; $**P<0.01$; $***P<0.001$.

diluted 10-fold and 1 μl used as template. Thermal cycling conditions were: 5 minutes 94°C, 25–33 cycles of 30 s at 94°C, 30 s at 60°C, and 1 minute at 72°C.

Oligonucleotides used were: mEdar S: 5′-GCACACTCATCCAGC ACTTC- 3′, mEdar AS: 5′-TTCTCCTCGTGTGTGTTAGC-3′; mGapd S: 5′-CGTAGACAAAATGGTGAAGGTCGG-3′, mGapd AS: 5′-AAG CAGTTGGTGGTGCAGGATG-3′; mKrt1-10 S: 5′-GCTTTGGTGGC GGTAGCTAT-3′, mKrt1-10 AS: 5′-TCAGCCTGAAGTCATCAGCT-3′; mKrt1-14 S: 5′-GGCCCAGATCCAGGAGATGAT-3′, mKrt1-14 AS: 5′-CAGGGGCTCTTCCAGCAGTATC-3′; mShh S: 5′-GCAGATATGA AGGGAAGATC-3′, mShh AS: 5′-CCAGTCGAAACCTGCTTCCA-3′.

Antibodies

Rat monoclonal antibodies were used to detect Integrin á6 (1:100 dilution; Serotec Ltd, Oxford, UK), CD34 (1:50; Pharmingen Laboratories, Franklin Lakes, NJ), and BrdU (1:100; Abcam, Cambridge, UK). Mouse monoclonal antibodies were used to detect Keratin 15 (1:100; Abcam), Nestin (1:200; Chemicon International Inc., Temecula, CA), and PCNA (1:200; Abcam). Polyclonal rabbit antibodies were used to detect Tenascin-C (1:200; Chemicon International Inc.), Keratin 14, and Keratin 6 (1:500; Covance Research Products, Denver, PA). Secondary antibodies used were either biotinylated goat anti-rabbit antibody (1:200; Vector Laboratories Inc., Burlingame, CA), biotinylated rabbit anti-rat antibody (1:200; Vector Laboratories Inc.), or Alexa Fluor® 488 goat anti-rabbit IgG (1:100; Invitrogen, Paisley, UK).

Immunostaining

For staining of sectioned tissue, skin samples were fixed overnight in 4% paraformaldehyde at 4°C, transferred to 70% ethanol, embedded in paraffin wax, and sectioned at 7 μm. Tissue sections were deparaffinized in xylene and rehydrated in graded alcohols. Antigen retrieval was performed by microwaving tissue sections in 10 mM sodium citrate (pH 6.0) for 1 minute, followed by 30 minutes incubation. When staining with mouse monoclonal antibodies, the MOM Basic kit (Vector Laboratories Inc.) was used. Otherwise, sections were blocked for 20 minutes in 5% normal goat serum. Primary antibodies were diluted in PBS and applied for 1 hour at room temperature. After washing in PBS, sections were incubated for 30 minutes at room temperature in secondary antibody and detected with either Vectastain ABC-peroxidase (Vector Laboratories Inc.) or Cy-3 streptavidin (1:100; Sigma Diagnostics Inc., St Louis, MO). Whole-mount immunostaining of tail epidermal sheets was performed as described (Braun *et al.*, 2003). Images were scanned using a confocal microscope from the dermal side toward the epidermal surface to a total thickness of 40–80 μm, which encompassed the epidermis from the HF bulb to the basal layer of IFE.

BrdU Labeling and Detection

To generate LRCs, the protocol described by Braun *et al.* (2003) was used. P10 littermates were given intraperitoneal injections of 50 μg BrdU/g body weight every 12 hours for a total of four injections and samples were collected 12 weeks later. Processed paraffin sections were incubated in 4 M HCl and washed in borate buffer. After blocking in 5% rabbit serum for 20 minutes, sections were incubated for 1 hour at room temperature with anti-BrdU antibody. Sections were incubated for 30 minutes at room temperature in secondary antibody and Vectastain ABC-peroxidase. For X-gal and BrdU double detection, tail skin from BrdU-labeled *Dct*::*lacZ* mice was immersed in X-gal staining solution for 5 hours prior to overnight fixation in 4% paraformaldehyde. Samples were then processed for BrdU detection.

Clonogenicity assays

Irradiated Swiss 3T3 fibroblasts (ATCC, Manassas, VA, catalog # 48-X) were seeded at a density of 250,000 cells per 60 mm culture dish in DMEM containing 10% fetal bovine serum and 1% penicillin/streptomycin/amphotericin (pen/strep/amp). Cells were allowed to attach to the dishes for 24 hours in 5% CO_2 at 37°C. Epidermal sheets were prepared by placing small skin pieces in 2 mg ml^{-1} Dispase (Invitrogen) in PBS at 37°C for 30 minutes. Following incubation, the epidermis was gently teased from the dermis as an intact sheet using fine forceps. Epidermal cells were dissociated by treatment in 0.25% trypsin for 10 minutes with agitation. Dissociated keratinocytes were suspended in keratinocyte serum-free media (Invitrogen), supplemented with 18% DMEM, 10% fetal bovine serum, 0.2% pen/strep/amp, 1 mM $CaCl_2$, 0.2 ng ml^{-1} human recombinant epidermal growth factor, and 25 μg ml^{-1} bovine pituitary extract, and 50,000 keratinocytes were seeded onto the feeder layers in each dish. Medium was changed twice weekly, beginning the second day after keratinocyte plating. After a 2-week culture, the dishes were rinsed with PBS and colonies were fixed with 10% formalin for 5 minutes and visualized by staining with 2% rhodamine B. A colony was defined as a cluster of 5 or more keratinocytes (Silva-Vargas *et al.*, 2005). For clonogenicity experiments involving E7 embryos, the entire yolk sac and embryo were trypsinized and plated. IFE and HF fractions were prepared from E18 tail skin essentially as described (Yi *et al.*, 2006). Freshly isolated tail skin was separated into IFE and dermis plus HF fractions by quickly and firmly tearing the IFE from the dermis using forceps. The dermal fraction, which contained the HFs, was placed in 0.2% collagenase for 30 minutes at 37°C. HFs were sedimented by centrifugation at 40 *g* for 5 minutes. HFs were washed twice with PBS and then HF and interfollicular epidermal fractions were dissociated into single cell suspensions using trypsin and used in clonogenicity assays. Each *n* represents an individual animal throughout. For analysis of clonogenic potential in prenatal skin, three independent litters were used for each time point.

Incisional wounding

Full-thickness, 1 cm longitudinal incisions were made to 8- to 10-week-old mice on the dorsal surface of the tail using a scalpel, starting 1 cm from where the tail meets the body. *Edaradd*$^{cr/+}$ animals were used as controls and were littermates of the *Edaradd*$^{cr/cr}$ mutants. All animals were observed to be healthy at the time of wounding and through the healing process. Three independent rounds of wounding were performed; $n = 10–15$ for each genotype. Experimental procedures were approved by the University of Manchester and the UK Home Office.

CONFLICT OF INTEREST

The authors state no conflict of interest.

ACKNOWLEDGMENTS

We thank I. Jackson, M. Dixon, D. Garrod, A. Hurlstone, M. Risley, and C. Thompson. This work was funded by Wellcome Trust Grant 075220/Z.

SUPPLEMENTARY MATERIAL

Figure S1. Expression of stem cell markers in WT postnatal tail epidermis.

Figure S2. Wound healing in dorsal trunk skin.

REFERENCES

Bishop GH (1945) Regeneration after experimental removal of skin in man. *Am J Anat* 76:153–81

Blanpain C, Lowry WE, Geoghegan A, Polak L, Fuchs E (2004) Self-renewal, multipotency, and the existence of two cell populations within an epithelial stem cell niche. *Cell* 118:635–48

Braun KM, Niemann C, Jensen UB, Sundberg JP, Silva-Vargas V, Watt FM (2003) Manipulation of stem cell proliferation and lineage commitment: visualisation of label-retaining cells in wholemounts of mouse epidermis. *Development (Cambridge, England)* 130:5241–55

Chmielowiec J, Borowiak M, Morkel M, Stradal T, Munz B, Werner S *et al.* (2007) c-Met is essential for wound healing in the skin. *J Cell Biol* 177:151–62

Clayton E, Doupe DP, Klein AM, Winton DJ, Simons BD, Jones PH (2007) A single type of progenitor cell maintains normal epidermis. *Nature* 446:185–9

Cotsarelis G (2006) Epithelial stem cells: a folliculocentric view. *J Invest Dermatol* 126:1459–68

Cotsarelis G, Sun TT, Lavker RM (1990) Label-retaining cells reside in the bulge area of pilosebaceous unit: implications for follicular stem cells, hair cycle, and skin carcinogenesis. *Cell* 61:1329–37

Coulombe PA (2003) Wound epithelialization: accelerating the pace of discovery. *J Invest Dermatol* 121:219–30

Fuchs E (2007) Scratching the surface of skin development. *Nature* 445: 834–42

Headon DJ, Emmal SA, Ferguson BM, Tucker AS, Justice MJ, Sharpe PT *et al.* (2001) Gene defect in ectodermal dysplasia implicates a death domain adapter in development. *Nature* 414:913–6

Ito M, Liu Y, Yang Z, Nguyen J, Liang F, Morris RJ *et al.* (2005) Stem cells in the hair follicle bulge contribute to wound repair but not to homeostasis of the epidermis. *Nat Med* 11:1351–4

Levy V, Lindon C, Harfe BD, Morgan BA (2005) Distinct stem cell populations regenerate the follicle and interfollicular epidermis. *Dev Cell* 9:855–61

Levy V, Lindon C, Zheng Y, Harfe BD, Morgan BA (2007) Epidermal stem cells arise from the hair follicle after wounding. *FASEB J* 21:1358–66

Li J, Chen J, Kirsner R (2007) Pathophysiology of acute wound healing. *Clin Dermatol* 25:9–18

Mackenzie MA, Jordan SA, Budd PS, Jackson IJ (1997) Activation of the receptor tyrosine kinase Kit is required for the proliferation of melanoblasts in the mouse embryo. *Dev Biol* 192:99–107

Morris RJ, Liu Y, Marles L, Yang Z, Trempus C, Li S *et al.* (2004) Capturing and profiling adult hair follicle stem cells. *Nat Biotechnol* 22:411–7

Morris RJ, Potten CS (1994) Slowly cycling (label-retaining) epidermal cells behave like clonogenic stem cells *in vitro*. *Cell Prolif* 27:279–89

Nijhof JG, Braun KM, Giangreco A, van Pelt C, Kawamoto H, Boyd RL *et al.* (2006) The cell-surface marker MTS24 identifies a novel population of follicular keratinocytes with characteristics of progenitor cells. *Development (Cambridge, England)* 133:3027–37

Nishimura EK, Jordan SA, Oshima H, Yoshida H, Osawa M, Moriyama M *et al.* (2002) Dominant role of the niche in melanocyte stem-cell fate determination. *Nature* 416:854–60

Papini R (2004) ABC of burns—management of burn injuries of various depths. *BMJ* 329:158–60

Rhee H, Polak L, Fuchs E (2006) Lhx2 maintains stem cell character in hair follicles. *Science* 312:1946–9

Rheinwald JG, Green H (1975) Serial cultivation of strains of human epidermal keratinocytes: the formation of keratinizing colonies from single cells. *Cell* 6:331–43

Schmidt-Ullrich R, Paus R (2005) Molecular principles of hair follicle induction and morphogenesis. *BioEssays* 27:247–61

Shirakata Y, Kimura R, Nanba D, Iwamoto R, Tokumaru S, Morimoto C *et al.* (2005) Heparin-binding EGF-like growth factor accelerates keratinocyte migration and skin wound healing. *J Cell Sci* 118:2363–70

Silva-Vargas V, Lo Celso C, Giangreco A, Ofstad T, Prowse DM, Braun KM *et al.* (2005) Beta-catenin and Hedgehog signal strength can specify number and location of hair follicles in adult epidermis without recruitment of bulge stem cells. *Dev Cell* 9:121–31

Taylor G, Lehrer MS, Jensen PJ, Sun TT, Lavker RM (2000) Involvement of follicular stem cells in forming not only the follicle but also the epidermis. *Cell* 102:451–61

Werner S, Grose R (2003) Regulation of wound healing by growth factors and cytokines. *Physiol Rev* 83:835–70

Werner S, Smola H, Liao X, Longaker MT, Krieg T, Hofschneider PH *et al.* (1994) The function of KGF in morphogenesis of epithelium and reepithelialization of wounds. *Science* 266:819–22

Yi R, O'Carroll D, Pasolli HA, Zhang Z, Dietrich FS, Tarakhovsky A *et al.* (2006) Morphogenesis in skin is governed by discrete sets of differentially expressed microRNAs. *Nat Genet* 38:356–62